ABUNDANCES IN TURNOFF STARS IN THE OLD, METAL-RICH OPEN CLUSTER, NGC 6791

ANN MERCHANT BOESGAARD[1,4], ELIZABETH E. C. JENSEN[2], AND CONSTANTINE P. DELIYANNIS[3,4]

[1] Institute for Astronomy, University of Hawaii at Manoa, 2680 Woodlawn Drive, Honolulu, HI 96822, USA; boes@ifa.hawaii.edu
[2] Department of Mechanical and Aerospace Engineering, Princeton University, Princeton, NJ 08544, USA; ejtwo@princeton.edu
[3] Department of Astronomy, Indiana University, 727 East 3rd Street, Swain Hall West 319, Bloomington, IN 47405-7105, USA; cpd@astro.indiana.edu

ABSTRACT

Open clusters have long been used to illuminate both stellar evolution and Galactic evolution. The oldest clusters, though rather rare, can reveal the chemical and nucleosynthetic processes early in the history of the Galaxy. We have studied two turnoff stars in the old, metal-rich open cluster, NGC 6791. The Keck + HIRES spectra have a resolution of ∼45,000 and signal-to-noise ratios of ∼40 per pixel. We confirm the high value for [Fe/H] finding +0.30 ± 0.08, in agreement with earlier results from evolved stars in other parts of the Hertzsprung–Russell diagram. We have also determined abundances for Na, Si, Ca, Ti, Cr, Ni, Y, and Ba. These are compared to a sample of old, metal-rich field stars. With the probable exception of enhanced Ni in the cluster stars, the field and cluster stars show similar abundances of the elements. Model predictions show that the Ni enhancement could result from enrichment of the pre-cluster gas by SN Ia. Orbital evidence indicates that NGC 6791 could have originated near the inner regions of the Galaxy where the metallicity is generally higher than it is in the disk or halo. Subsequent perturbations and migrations may have resulted in its current heliocentric distance of 4 kpc and 1 kpc above the Galactic plane.

Key words: open clusters and associations: individual (NGC 6791) – stars: abundances – stars: evolution – stars: late-type – stars: Population II

1. INTRODUCTION

The study of open clusters has greatly advanced our understanding of stellar evolution through comparisons between observations and theoretical models. The distribution of stars in the Hertzsprung–Russell (H–R) diagram has been an especially useful tool in this regard. Comparing clusters of different ages via the turnoff points, as shown initially by, e.g., Johnson & Sandage (1955) and Sandage (1956), has proven to be extremely important. Open clusters have also been used to increase our knowledge of cluster and Galactic dynamics, the distance scale of the universe, and the chemical history of the Galaxy.

Stars within a particular cluster are thought to have been formed together, within a few Myr, and share the same composition and space motion. Comparative composition studies have mostly been limited to Fe and Li, however. See Friel et al. (2002) for a presentation of metallicities and kinematics for 39 old open clusters (older than 0.8 Gyr). However, it is important to study a full range of elements including CNO and other alpha elements, Fe-peak elements, and n-capture elements. Cluster-to-cluster comparisons can reveal possible trends with age. Comparisons between dwarfs and giants reveal potential mixing that could alter the surface abundances in the evolved giants. Such comparisons have been done for globular clusters providing interesting insights into their evolution, but open clusters have not yet received such comprehensive studies. Old clusters are especially interesting as they are nearly as old as the Galactic disk.

Ages can be determined for open clusters and they are found to span the lifetime of the Galactic disk. Open clusters that are old are relatively rare because old clusters are subject to dissipation after several passages through the disk plane such that former cluster members become part of the general field. The field stars of Chen et al. (2003) and Feltzing & Gonzales

(2001) that are old and metal-rich could be the remnants of similar, but less massive, clusters like NGC 6791. The extant old clusters tend to probe the outer regions of the Galaxy and are good tracers of Galactic chemical evolution. Current evidence seems to point to a rapid, early chemical enrichment of the disk, plus infall of some metal-poor gas (e.g., Friel et al. 2002). This picture comes from abundances of Fe only. A much fuller picture would require abundances for an array of elements since different mass ranges of stars produce different nucleosynthetic products.

The old open clusters contain the clues to early chemical evolution in the atmospheres of their unevolved stars. Unlike many of the giant stars, their atmospheres are not contaminated by the products of nuclear reactions in the interiors.

2. NGC 6791

The cluster, NGC 6791, is an enigmatic open cluster. It is unusually massive; apparently its metallicity is at least a factor of 2 higher than the Sun's, yet it is very old. In addition, it has extreme kinematics and is about 1 kpc above the Galactic plane. This cluster defies many of the existing paradigms about the formation of the Galaxy and its chemical history. Thus, it is especially important to determine the details of its chemical composition.

NGC 6791 is anomalous in several respects: (1) typical open clusters contain a few hundred stars, but NGC 6791 is very populous with a mass of ∼4000 $M_\odot$ (Carraro et al. 2006; Gratton et al. 2006). (2) It is apparently super metal-rich with [Fe/H] ∼+0.4—but this has been determined only from its evolved stars (Peterson & Green 1998; Worthey & Jowett 2003; Gratton et al. 2006; Carraro et al. 2006). (3) In spite of being metal-rich, it is very old; the photometry is excellent (Montgomery et al. 1994) and the H–R diagrams yield ages of 8–10 Gyr (Demarque et al. 1992; Garnavich et al. 1994; Montgomery et al. 1994; Chaboyer et al. 1999). Other old open clusters include M67 and NGC 188 which have solar metallicity and ages of 4–7 Gyr. (4) It

clearly does not fit any age–metallicity relation for the Galactic disk given its very old age and unusually high metallicity (e.g., Carraro et al. 2006). (5) The combination of its heliocentric distance of ~4 kpc (King et al. 2005) and its Galactic latitude of +11°, means it is ~1 kpc above the Galactic plane, far above the disk where open clusters reside. (6) Given its high metallicity and its distance from the Galactic center (Bedin et al. 2006), it does not fit any radial abundance gradient for the Galaxy (e.g., Carraro et al. 2006). (7) It has an atypical white dwarf cooling curve (Bedin et al. 2005).

Photometry of NGC 6791 has been done by Kinman (1965), Kaluzny (1990), Montgomery et al. (1994; hereafter MJP), Kaluzny & Rucinski (1995), Stetson et al. (2003), Carney et al. (2005), and Anthony-Twarog et al. (2007). Isochrone fitting in the color–magnitude diagram indicates both high metal content and an old age for NGC 6791.

The high metal content has been confirmed by spectroscopic studies. The Fe abundances that have been found so far for this cluster are from evolved stars. The first spectroscopic alert that the cluster showed high metallicity came from Peterson & Green (1998) who observed one blue horizontal branch star at medium–high resolution (20,000) with the echelle spectrograph on the NOAO/KPNO 4 m Mayall telescope. They found a temperature of 7300 ± 50 K and $\log g = 3.6 \pm 0.2$ dex resulting in an iron abundance of [Fe/H] $= +0.4 \pm 0.1$ dex. Based on the proper motion and radial velocity their star is a confirmed member of the cluster. Worthey & Jowett (2003) looked at 24 giant stars at medium–low resolution (~2200) with the MDM 2.4 m telescope. Their mean iron abundance is [Fe/H] $= 0.320 \pm 0.023$ dex. Gratton et al. (2006) observed four red giant clump stars at a resolution 29,000 with the SARG spectrograph on the Galileo National Telescope. They found [Fe/H] $= +0.47 (\pm 0.04,$ rms $= 0.08)$ dex. Carraro et al. (2006) used HYDRA on the WIYN telescope to obtain echelle spectra of 10 giant stars with a resolution of 20,000 and found the metal abundance to be [M/H] $= +0.39 \pm 0.05$.

Recent work from deep imaging with *Hubble Space Telescope* second epoch observations have allowed the determination of the cluster's proper motion and orbit (Bedin et al. 2006). According to these authors, this cluster had its origin in the inner regions of the Galaxy. It has come within 3 kpc of the Galactic center and has crossed the disk in regions of high stellar density. The cluster has survived because of its high stellar mass and density. The orbit has an unusually high eccentricity for an open cluster, $\epsilon \sim 0.5$. It travels to an outer distance from the Galactic center of ~10 kpc.

In this work, we have determined abundances of several elements in two "unevolved" main-sequence turnoff stars. Their surface composition is unaltered by nuclear fusion products and subsequent mixing, which affects the red giant and horizontal branch stars. Our stars represent the original composition of the stars and the cluster, with the potential exception of the effects of microscopic diffusion. Richard et al. (2002) have studied the effects of gravitational settling, thermal diffusion, and radiative acceleration on the surface composition of metal-poor stars with models with [Fe/H] from -4.31 to -0.71; they have shown that the effects for globular cluster turnoff stars are much smaller in the higher metallicity models. Michaud et al. (2004) suggest that turnoff stars may show small underabundances relative to the initial abundances. For the open cluster M67 at 3.7 Gyr, they calculate that [Fe/H] may be down by -0.03 dex and [Ti/H] down by -0.02 at 5800 K in turnoff stars. For the open cluster NGC 188 with an older age of 6.7 Gyr, they find that [Fe/H] may
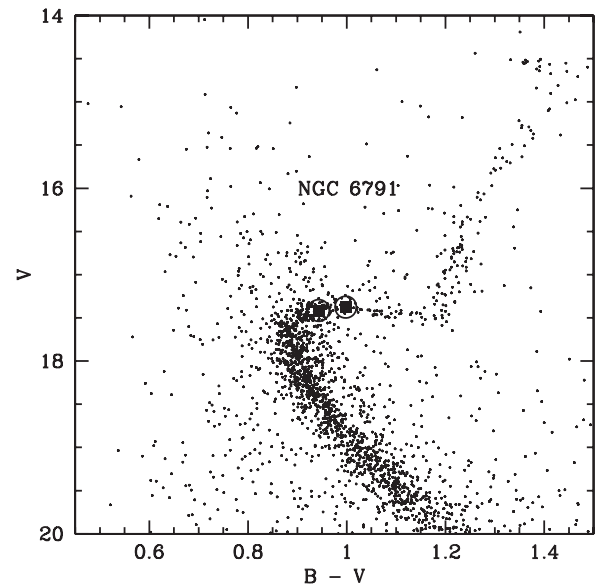

Figure 1. Color–magnitude diagram of NGC 6791 from the photometry of MJP. The two turnoff stars that we observed are indicated by the large circles.

be down by -0.05 dex and [Ti/H] by -0.04 dex. Our cluster, NGC 6791, is 8–10 Gyr in age and would have had more time for microscopic diffusion to have taken place. Still, the effects at 5800 K are small and even smaller at lower temperatures.

3. OBSERVATIONS

Figure 1 shows the H–R diagram with the photometry of MJP where the positions of the two stars we observed are indicated by large circles. We have obtained high-resolution, high signal-to-noise (S/N) echelle spectra from the Keck I 10 m telescope with the original HIRES (Vogt et al. 1994) of those two turnoff stars in NGC 6791: MJP 4112 and MJP 5061. The turnoff stars are faint at $V \sim 17.4$, so long integrations were needed even on the largest telescope. The data were obtained on two observing runs, 1999 June 7 and 8 and 2000 May 28 and 29 (UT). A log of the observations is presented in Table 1. The individual integration times were 40–60 minutes with a total of 4 hr on MJP 4112 and 3 hr on MJP 5061. The spectral resolution is ~45,000 and the S/N ~40 per pixel. Exposures were made of 15 internal flat fields and 15 bias spectra; comparison spectra of Th–Ar were obtained at the beginning and end of each of the four nights.

We conducted standard data reduction procedures in IRAF. The images were first bias-subtracted. A master-flat field was created by median-combining all of the flats and then normalized using the routine *flatnormalize*. The images were then divided by the master flat and cosmic-ray events were removed. The spectra, including the Th–Ar comparisons were traced and extracted. The wavelength solution from the Th–Ar spectra

Table 1
Keck HIRES Observations

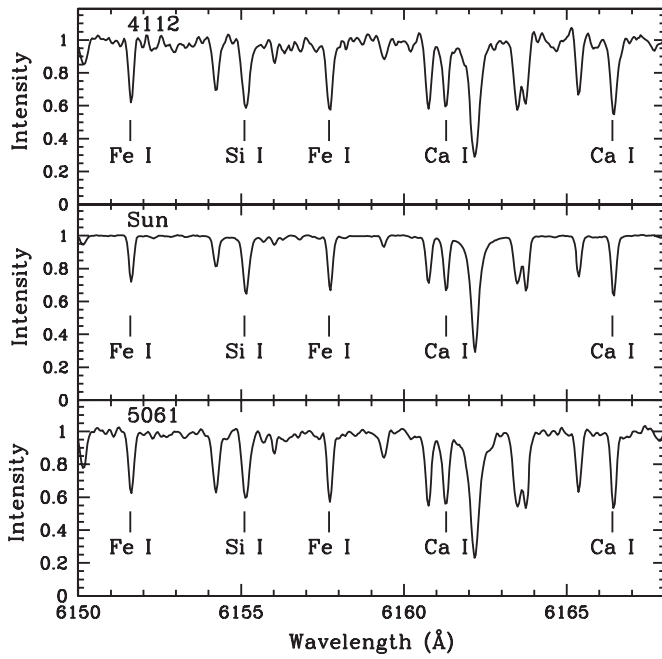| Star	V	$B-V$	Night	Exp. Time (minutes)	S/N	Total S/N
4112	17.415	0.943	2000 May 28	120	30	
			2000 May 29	120	24	38
5061	17.375	0.998	1999 Jun 7	80	25	
			1999 Jun 8	100	31	40

Figure 2. Sample spectral regions of each star along with a 10 s exposure of the spectrum of the Moon taken with HIRES on 2003 January 11. Lines of Si I, Ca I, and Fe I are indicated. MJP 4112 is hotter than the Sun at 5800 K, while MJP 5061 is cooler at 5650 K; note that the lines are stronger in both the hotter and the cooler star in NGC 6791 relative to solar.

was applied to the individual star spectra, and then the spectra were corrected for their radial velocity shifts. The multiple exposures for the individual stars were median combined and the continuum level was found by fitting a high-order spline3 function to the individual orders. Figure 2 shows a sample of the reduced, combined spectra of each star near 6160 Å. Lines of Ca I, Si I, and Fe I are indicated. We took a 10 s exposure of the spectrum of the Moon, as a solar surrogate, with the same equipment on 2003 January 11; this is shown for comparison in the middle panel of the figure. The lines in both cluster stars are clearly stronger than the solar lines.

We measured equivalent widths of nearly 140 lines in each star over several orders, mostly between 5900 and 6800 Å because there was considerable blending at shorter wavelengths. The measurements were made in IRAF with the *splot* package with Gaussian profile fitting. We measured lines of the alkali element, Na (Na I), the α-fusion elements, Si, Ca, Ti (Si I, Ca I, Ti I), the Fe peak elements, Cr, Fe, Ni (Cr I, Cr II, Fe I, Fe II, Ni I), and the neutron-capture elements, Y (Y II) and Ba (Ba II). A table of these line measurements, along with the species, wavelengths, lower excitation potentials, and oscillator strengths (log gf) values is available in the Appendix as Table A1.

4. ABUNDANCES

4.1. Stellar Parameters

Due to the low galactic latitude, 11°, and large distance, ~4000 pc, of NGC 6791, reddening is a problem. And due to the high metallicity of NGC 6791, it is difficult to calibrate the reddening effects. That results in an uncertain reddening correction. In fact, published values range from $E(B - V) =$ 0.10 (Janes 1984) to 0.22 (Kinman 1965). Liebert et al. (1994) found $E(B - V) = 0.135$, Chaboyer et al. (1999) concluded that the reddening is between 0.08 and 0.13, while Anthony-

Table 2
Model Parameters

Star	T_{eff} (K)	log g	[Fe/H]	ξ (km s^{-1})
MJP 4112	5800	4.3	+0.3	1.35
MJP 5061	5650	4.3	+0.3	1.23

Twarog et al. (2007) found $E(B - V) = 0.155 \pm 0.016$ based on Strömgren photometry. The latter authors point out that the usual calibrations are likely to underestimate the colors of turnoff stars with high metallicity. The uncertainty in the reddening and in the calibrations means that temperatures determined from color indices will be uncertain. Therefore, we did not try to determine temperatures from $(B - V)$ or other color indices. We chose to find T_{eff} spectroscopically by making use of the plentiful lines of Fe I. Thus, we avoided the problems with the effect of interstellar reddening on the colors and thus the temperatures derived from them. We point out, however, that the model atmospheres will be uncertain due to the high metallicity and this may introduce some systematic errors.

For the temperature determinations we used ~35 Fe I lines ranging in excitation potential from 0.86 to 4.83 eV. We tried to determine values for log g from comparison of abundances found from Fe I and Fe II and from Cr I and Cr II; however, there were few usable lines of either Fe II and Cr II. We settled on log g of 4.3 which gave a good compromise for Fe and Cr in MJP 5061 for the agreement for the two ions in the two elements. We used the same value for log g for MJP 4112 based on the similarity of the positions of the two stars in the color–magnitude diagram. We calculated the microturbulent velocity, ξ, from the empirical formula involving T_{eff} and log g from Edvardsson et al. (1993); this relationship is not validated in stars of such high metallicity, but our results are not overly sensitive to the value of the microturbulent velocity. The stellar parameters we used for the model atmospheres are given in Table 2.

4.2. Elemental Abundances

We employed MOOG (2002 version) to determine abundances of several elements via the *abfind* driver. The grid of model atmospheres of Kurucz was interpolated to find the model atmosphere for each star. We started with models with [Fe/H] = +0.4, but it became apparent that the abundance of Fe was closer to +0.3, so we rederived all the abundances with that value for [Fe/H] in the models. Abundances were determined for each ion. For elements with more than one ion, the final abundance was determined as weighted by the number of lines used. For Ba the hyperfine structure was included in the line input data and the *blends* driver was used in MOOG. The results can be found in Table 3. The standard deviations from the internal agreements from individual lines are given there.

We were unable to derive an abundance for Li because the line at 6707.45, presumably due to Fe I, was much stronger than the Li feature in the blend due to the high value of [Fe/H]. An attempt at spectrum synthesis of the feature was unsuccessful due to the weakness of the Li doublet and the noise in the spectra; we were able to obtain a satisfactory fit to the three Fe I lines in the region: $\lambda\lambda$6703, 6705, 6710 in both stars.

We determined abundance errors that result from the uncertainties in the model parameters by running additional models which varied T_{eff} by 100 K, varied log g by 0.2 dex, [Fe/H] by 0.1 dex and ξ by 0.2 km s^{-1}. Tables 4 and 5 show those errors for each parameter for each ion in each star.

Table 3
Abundances Results

MJP 4112				MJP 5061			
Ion	Abund.	No. of Lines	St. Dev.	Ion	Abund.	No. of Lines	St. Dev.
Na I	6.78	2	±0.03	Na I	6.63	2	±0.10
Si I	8.02	7	±0.17	Si I	7.91	6	±0.13
Ca I	6.67	19	±0.12	Ca I	6.59	23	±0.16
Ti I	5.43	15	±0.21	Ti I	5.36	15	±0.17
Cr I	6.00	15	±0.16	Cr I	5.91	14	±0.18
Cr II	6.29	3	±0.13	Cr II	5.96	4	±0.07
Cr	6.05	18	⋯	Cr	5.92	18	⋯
Fe I	7.78	32	±0.14	Fe I	7.84	35	±0.13
Fe II	7.97	5	±0.06	Fe II	7.76	4	±0.03
Fe	7.81	37	⋯	Fe	7.83	39	⋯
Ni I	6.68	19	±0.15	Ni I	6.75	24	±0.14
Y II	2.47	3	±0.34	Y II	2.66	3	±0.14
Ba II	2.31	3	±0.09	Ba II	2.49	2	±0.25

Table 4
Abundance Errors for MJP 4112

Ion	$T = \pm 100$ K	$\log g = \pm 0.2$	[Fe/H] $= \pm 0.1$	$\xi = \pm 0.2$
Na I	±0.05	∓0.03	±0.00	∓0.02
Si I	±0.02	∓0.02	±0.01	∓0.02
Ca I	±0.07	∓0.06	±0.02	∓0.04
Ti I	±0.10	∓0.03	±0.00	∓0.07
Cr I	±0.10	∓0.05	±0.01	∓0.07
Cr II	∓0.04	±0.03	±0.03	∓0.08
Fe I	±0.08	∓0.03	±0.01	∓0.07
Fe II	∓0.07	±0.03	±0.06	∓0.04
Ni I	±0.06	∓0.02	±0.01	∓0.05
Y II	±0.00	±0.05	±0.04	∓0.10
Ba II	±0.01	±0.01	±0.04	∓0.08

Table 5
Abundance Errors for MJP 5061

Ion	$T = \pm 100$ K	$\log g = \pm 0.2$	[Fe/H] $= \pm 0.1$	$\xi = \pm 0.2$
Na I	±0.05	∓0.03	±0.01	∓0.01
Si I	±0.00	∓0.01	±0.02	∓0.01
Ca I	±0.07	∓0.06	±0.02	∓0.03
Ti I	±0.11	∓0.03	±0.01	∓0.05
Cr I	±0.10	∓0.04	±0.02	∓0.05
Cr II	∓0.04	±0.04	±0.03	∓0.04
Fe I	±0.07	∓0.03	±0.02	∓0.04
Fe II	∓0.06	±0.06	±0.04	∓0.03
Ni I	±0.05	∓0.02	±0.02	∓0.03
Y II	±0.00	±0.06	±0.04	∓0.07
Ba II	±0.02	±0.01	±0.06	∓0.08

5. RESULTS

The abundance ratios that we derived are presented in Table 6. The 1σ errors given in that tables are the result of adding the errors in Tables 4 and 5 in quadrature. (They do not include uncertainties in the equivalent width measurements.) The cluster mean, the average for the two stars, is also given in Table 6 with the 1σ error taken from the individual errors as divided by the square root of 2.

Our Fe abundances confirm the high Fe content found in the evolved stars in NGC 6791—giants and a horizontal branch star—from lower resolution spectroscopy. Based on 32 Fe I lines and five Fe II, lines we find log N(Fe/H) = 7.81 and [Fe/H] = 0.29 ± 0.11 for MJP 4112. For MJP 5061 we used 36 Fe I lines and four Fe II to find log N(Fe/H) = 7.83 and [Fe/
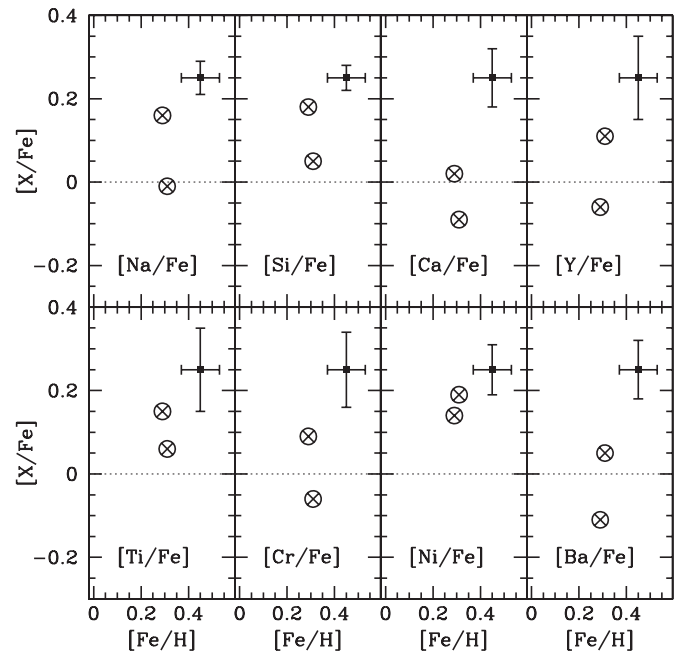

Figure 3. Abundance ratios relative to Fe in the two stars of NGC 6791. The 1σ errors due to uncertainties in the stellar parameters for the cluster mean are shown for each element ratio. Within the errors the ratios [X/Fe] are ~0.0 for the cluster mean with the probable exception of Ni.

H] = 0.31 ± 0.11. The average for the two turnoff stars is thus [Fe/H] = 0.30 ± 0.08. (For solar log N(Fe/H), we adopt the value used in the MOOG program from Anders & Grevesse 1989 of 7.52.)

In addition, we have found elemental abundances for eight other elements. Figure 3 shows the abundances in our two stars as normalized to Fe, i.e., [X/Fe], plotted against their values of [Fe/H] for those eight elements. The cluster mean error bars are shown in the upper right of each panel. Within that error we see that the alkali metal, [Na/Fe], and the alpha elements, [Si/Fe], [Ca/Fe], and [Ti/Fe], are near 0.0, i.e., normal. The neutron-capture elements, [Y/Fe] and [Ba/Fe], also appear to be normal. That is, those elements are enhanced as much as Fe is enhanced relative to solar. The Fe-peak element, Cr, is also in alignment with Fe. However, both stars seem to have enhanced values of [Ni/Fe], another Fe-peak element.

We can compare our results with those of field star samples that are both old and metal-rich. In the Edvardsson

Table 6
Abundances Ratios and Errors

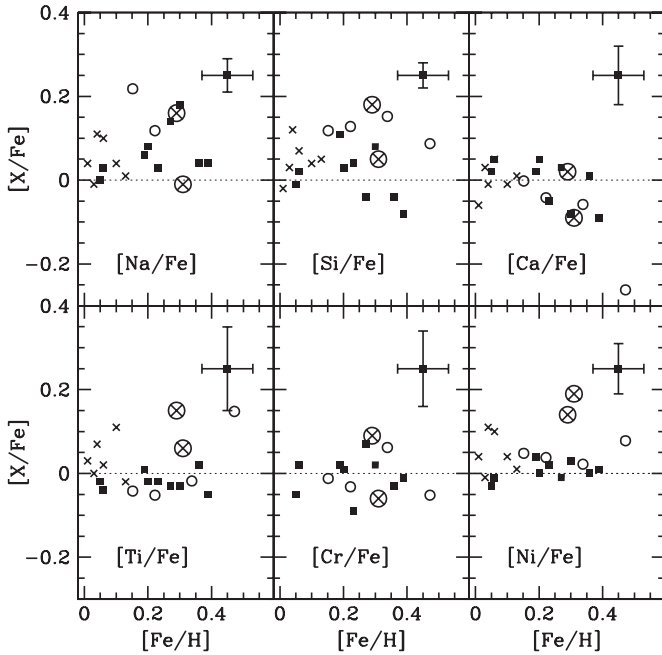| MJP 4112			MJP 5061			Cluster	
Element	Abund.	σ	Element	Abund.	σ	Mean	σ
[Fe/H]	+0.29	±0.11	[Fe/H]	+0.31	±0.11	+0.30	±0.08
[Na/Fe]	+0.16	±0.06	[Na/Fe]	−0.01	±0.06	+0.07	±0.04
[Si/Fe]	+0.18	±0.04	[Si/Fe]	+0.05	±0.03	+0.11	±0.03
[Ca/Fe]	0.02	±0.10	[Ca/Fe]	−0.09	±0.10	−0.03	±0.07
[Ti/Fe]	+0.15	±0.13	[Ti/Fe]	+0.06	±0.14	+0.10	±0.10
[Cr/Fe]	+0.09	±0.12	[Cr/Fe]	−0.06	±0.13	+0.01	±0.09
[Ni/Fe]	+0.14	±0.08	[Ni/Fe]	+0.19	±0.08	+0.17	±0.06
[Y/Fe]	−0.06	±0.12	[Y/Fe]	+0.11	±0.14	+0.03	±0.10
[Ba/Fe]	−0.11	±0.09	[Ba/Fe]	+0.05	±0.10	−0.03	±0.07

Figure 4. Comparison of the abundance results in our turnoff stars in NGC 6791 with old, metal-rich field stars. Our data are the large circled crosses. The small crosses are from Edvardsson et al. (1993), the open circles are from Feltzing & Gonzales (2001), and the filled squares are from Chen et al. (2003). Those field stars are all older than 8 Gyr. The two cluster stars fall in the same region as the field stars, with the probable exception of [Ni/Fe] which is nearly 3σ above 0.0. Certainly, the cluster mean values from Table 6 are completely consistent with the field stars, except for Ni. The 1σ errors due to uncertainties in the stellar parameters are shown for each element ratio and refer only to our stars.

et al. (1993) sample of 189 disk stars, there are six stars that are older than 8.5 Gyr with [Fe/H] = +0.01 to +0.13. In the spectral abundance analysis of old, metal-rich disk field stars of Chen et al. (2003), there are nine stars with ages > 8 Gyr and with [Fe/H] values from +0.05 to +0.47. In addition, Feltzing & Gonzales (2001) have four stars that are older than 8 Gyr and a range in [Fe/H] from +0.15 to +0.47. The elements in common in our analysis and those studies are Na, Si, Ca, Ti, Cr, and Ni, although Cr was not done by Edvardsson et al. (1993). This comparison is shown in Figure 4. Our NGC 6791 turnoff stars are remarkably similar to those old, metal-rich field stars. The ratio, [Na/Fe], is near 0.0 in NGC 6791 and in most of the field stars. The alpha-element ratios, [Si/Fe], [Ca/Fe], and [Ti/Fe], show agreement between the field and cluster stars. The Fe-peak element, Cr, should be near 0.0 and it is within the errors. Compared to those old, metal-rich stars, the cluster value for [Ni/Fe] is above 0.00 by 0.17 ± 0.06 dex.

In disk and halo field stars, the alpha elements, Mg, Si, Ca, Ti show enhancements in stars with lower metallicities (e.g., Edvardsson et al. 1993; Stephens & Boesgaard 2002), but these four elements usually share similar enhancements. There is, however, generally more scatter in the [Ti/Fe] values at a given [Fe/H], for example see Figure 18 in Stephens & Boesgaard (2002) which shows the four alpha elements and includes the results of Edvardsson et al. (1993). There is a range of ~0.3 dex in [Ti/Fe] for field stars—of all ages—in the Edvardsson et al. (1993) sample with [Fe/H] > 0.0. The mild enhancement in [Ti/Fe] that may be present in the NGC 6791 stars could result from a combination of our errors and an intrinsic scatter in this alpha-product element.

The apparent Ni enhancement could be the result of the contribution of SN Ia to the pre-cluster gas. The models of exploding CO white dwarfs of Tsujimoto et al. (1995) predict that the mass of Ni/Fe that is synthesized could be a factor of 2 higher than the solar ratio.

As we point out in Section 2, NGC 6791 does not fit any age–metallicity relation in the Galactic disk. Furthermore, the old, metal-rich field stars, which we have used for our comparison sample in Figure 4, do not fit the age–metallicity relationship either. Furthermore, as Carraro et al. (2006) point out, NGC 6791 does not fit a radial abundance gradient in the Galaxy. The existence of such a cluster indicates that there were complex beginnings and subsequent evolution of our Galaxy. The orbital solution for the cluster of Bedin et al. (2006) indicates that it could have been formed in the inner regions of the Galaxy. Inasmuch as the Galactic bulge is metal-rich—presumably due to rapid early star formation and chemical enrichment—the formation of NGC 6791 in that region could account for the enhancement of our element abundances. Only because of its high cluster mass and large stellar density has NGC 6791 survived through several crossings of the Galactic disk.

6. SUMMARY AND CONCLUSIONS

NGC 6791 is an exotic open cluster in part because its metallicity is at least a factor of 2 higher than solar, yet it is very old. Other old open clusters such as M67 and NGC 188 with ages of 4–7 Gyr are not metal-rich but seem to have solar or near-solar composition. With its mass of ~4000 $M_\odot$, NGC 6791 is especially massive for an open cluster.

Previous determinations of the metallicity of NGC 6791 have been of evolved stars because the main-sequence stars are faint and the available telescopes of 4–5 m in diameter. We have been able to obtain high-resolution spectra of two unevolved turnoff stars with the Keck I 10 m telescope with HIRES.

Due to the great distance and low Galactic latitude of NGC 6791 and the consequent large (and uncertain) value for the reddening, we relied on our spectra for the stellar parameter determination. In addition to finding the abundance of Fe, we have determined abundances for Na, Si, Ca, Ti, Cr, Ni, Y, and Ba.

We have compared our abundance results for our turnoff stars with a sample of 19 old (age > 8 Gyr), metal-rich ([Fe/H] > +0.01) field stars from the literature. The abundance ratios in the cluster and those field stars are very similar, with the probable exception of [Ni/Fe]. An enhancement in Ni could result from a surfeit of SN Ia explosions in the pre-cluster gas. Grenon (1999) has studied the origin and kinematics of super-metal-rich stars ([M/H] > +0.30) that are 10 Gyr old and suggests that they formed close to the bulge and, through perturbations by the bar of the Galaxy, were driven to greater distances from the center. This could be the case for our cluster and for the 19 field comparison stars. The orbits calculated by Bedin et al. (2006) indicate that NGC 6791 has a perigalacticon of ~3 kpc, an apogalacticon of ~10 kpc, and a *boxy* type orbit with a high eccentricity, ~0.5: unusual for an open cluster.

In any case, it seems clear that the formation and history of the Galaxy and the Galactic disk were not simple, straightforward processes. The beginnings for galactic structure and chemical evolution must have been complex. NGC 6791 is an example of this complexity: massive for an open cluster, old yet super-metal-rich, an eccentric orbit, currently a kpc above the Galactic plane, yet having undergone several passages through the disk, inconsistent with any radial abundance gradient and in defiance of any age–metallicity relation.

APPENDIX

Table A1
Measured Equivalent Widths

λ	Ex. Pot.	$\log gf$	Equivalent Widths	
(Å)	(eV)		MJP 4112	MJP 5061
Na I				
6154.230	2.10	−1.66	69.7	55.8
6160.753	2.10	−1.35	93.8	96.0
Si I				
5772.148	5.08	−1.75	90.8	⋯
5948.545	5.08	−1.225	121.6	110.3
6125.026	5.61	−1.48	52.5	70.3
6142.490	5.62	−1.48	77.6	54.5
6145.020	5.61	−1.37	59.1	55.5
6155.141	5.62	−0.84	121.0	112.0
6243.820	5.61	−1.27	105.7	85.5
Ca I				
4512.270	2.52	−1.90	37.6	57.6
4526.934	2.71	−0.49	146.1	126.9
4685.268	2.93	−1.88	95.5	85.2
5260.389	2.52	−1.72	67.3	69.1
5261.707	2.52	−0.6545	121.7	129.1

Table A1
(Continued)

λ	Ex. Pot.	$\log gf$	Equivalent Widths	
(Å)	(eV)		MJP 4112	MJP 5061
5262.241	2.52	−0.60	141.5	161.6
5512.980	2.93	−0.3685	134.6	119.7
5581.968	2.52	−0.56	⋯	131.6
5590.117	2.52	−0.6405	127.9	113.8
5594.466	2.52	0.023	189.6	⋯
5598.480	2.52	−0.22	⋯	172.5
5857.451	2.93	0.235	⋯	171.1
6122.217	1.89	−0.32	232.6	246.5
6161.300	2.52	−1.27	99.7	104.2
6162.173	1.90	−0.09	264.2	261.5
6163.755	2.52	−1.286	⋯	100.0
6166.440	2.52	−1.14	⋯	97.1
6169.042	2.52	−0.797	132.6	116.1
6169.562	2.53	−0.374	157.0	145.8
6449.810	2.52	−0.502	142.0	146.9
6455.600	2.52	−1.34	97.5	96.2
6462.569	2.52	0.286	288.3	285.4
6471.688	2.52	−0.690	132.2	135.7
6499.650	2.52	−0.818	120.1	124.5
Ti I				
4518.023	0.826	−0.269	119.8	⋯
4533.239	0.848	0.532	178.1	150.6
4534.778	0.836	0.336	⋯	144.8
4617.254	1.749	0.445	85.7	⋯
4840.874	0.900	−0.453	82.8	102.5
4981.732	0.848	0.560	153.1	⋯
4991.067	0.836	0.436	⋯	155.3
4999.504	0.826	0.306	146.7	140.2
5016.162	0.848	−0.518	108.8	98.8
5020.028	0.836	−0.358	⋯	118.2
5022.871	0.826	−0.378	111.6	110.9
5036.468	1.443	0.186	⋯	95.3
5039.959	0.021	−1.130	⋯	122.8
5064.654	0.048	−0.855	⋯	136.9
5192.969	0.021	−0.950	107.3	126.6
5953.170	1.890	−0.310	74.5	77.1
5978.540	1.870	−0.440	71.2	⋯
6126.224	1.070	−1.320	56.2	61.6
6258.110	1.440	−0.430	72.2	93.1
6261.106	1.430	−0.480	77.3	⋯
6303.760	1.440	−1.600	27.0	⋯
Cr I				
4511.900	3.0900	−1.150	65.8	71.5
4545.945	0.9415	−1.370	100.2	⋯
4591.389	0.9685	−1.740	⋯	89.6
4600.741	1.0037	−1.260	130.9	101.4
4616.120	0.9829	−1.190	112.9	134.5
4626.174	0.9685	−1.320	115.4	107.4
4651.282	0.9829	−1.460	117.3	103.6
4652.152	1.0037	−1.030	124.8	140.7
4789.350	2.5400	−0.366	80.7	80.3
5206.038	0.9415	0.019	385.4	⋯
5247.566	0.9610	−1.640	107.9	122.5
5296.691	0.9829	−1.400	128.9	124.5
5298.277	0.9829	−1.160	⋯	162.3
5329.170	2.9100	−0.064	98.6	⋯
5345.801	1.0037	−0.980	178.6	175.0
5348.312	1.0037	−1.290	142.0	136.1
5409.772	1.0301	−0.715	192.2	⋯
6330.100	0.940	−2.94	⋯	58.2
Cr II				
4558.650	4.0737	−0.660	⋯	85.9

Table A1
(Continued)

λ (Å)	Ex. Pot. (eV)	log gf	Equivalent Widths MJP 4112	MJP 5061
4588.199	4.0715	−0.630	· · ·	87.9
4634.070	4.0725	−1.240	82.0	· · ·
4848.235	3.8647	−1.140	87.6	79.3
5237.329	4.0737	−1.160	90.5	62.3
Fe I				
5916.247	2.450	−2.9900	· · ·	90.6
5934.655	3.930	−1.0200	114.8	106.5
5956.700	0.860	−4.5640	78.9	86.1
6024.058	4.550	−0.0600	135.2	139.0
6027.048	4.076	−1.1495	103.4	88.6
6055.992	4.734	−0.4600	99.4	93.9
6065.481	2.609	−1.4700	156.8	160.0
6078.999	4.652	−1.1200	· · ·	75.5
6082.720	2.220	−3.5330	65.5	68.7
6127.904	4.143	−1.3990	63.2	75.0
6136.615	2.453	−1.4050	171.8	· · ·
6137.691	2.588	−1.3745	181.8	193.5
6151.618	2.176	−3.2990	71.4	75.4
6157.725	4.076	−1.2600	· · ·	87.1
6165.360	4.140	−1.4700	66.1	73.5
6173.341	2.223	−2.8800	96.3	102.2
6180.203	2.728	−2.6225	81.9	94.8
6187.990	3.940	−1.5700	74.5	81.7
6219.280	2.198	−2.4330	110.5	· · ·
6230.723	2.559	−1.2785	183.6	230.1
6246.318	3.603	−0.8770	156.4	162.9
6252.555	2.404	−1.7270	150.0	165.7
6265.140	2.180	−2.5100	107.9	126.4
6297.800	2.220	−2.7000	97.1	118.1
6335.330	2.198	−2.2035	119.1	133.1
6355.029	2.85	−2.358	82.6	· · ·
6380.742	4.187	−1.3875	86.5	82.7
6393.601	2.433	−1.5760	171.8	176.0
6411.649	3.650	−0.6600	149.7	177.4
6469.193	4.830	−0.6200	98.3	90.1
6481.869	2.279	−2.9840	90.7	105.7
6498.940	0.958	−4.6946	· · ·	86.5
6592.913	2.728	−1.5365	· · ·	153.8
6593.868	2.433	−2.3940	· · ·	125.7
6597.561	4.795	−0.9200	65.3	75.6
6609.109	2.559	−2.6765	97.1	102.1
6750.152	2.424	−2.6080	93.4	104.2
6752.707	4.640	−1.2000	57.9	69.1
Fe II				
6084.100	3.20	−3.810	39.9	· · ·
6113.322	3.22	−4.160	27.2	· · ·
6149.249	3.89	−2.9300	· · ·	44.8
6247.562	3.89	−2.7240	80.3	62.1
6369.460	2.89	−4.16	38.5	26.2
6456.391	3.90	−2.3290	90.4	79.0
Ni I				
4714.408	3.3801	0.2300	· · ·	229.5
4715.757	3.5435	−0.3400	108.0	143.4
4756.510	3.4802	−0.3400	106.3	· · ·
4786.531	3.4198	−0.1700	· · ·	131.9
4831.169	3.6063	−0.4200	86.2	97.2
4904.407	3.5424	−0.1700	129.7	155.6
4937.341	3.6063	−0.3900	· · ·	129.1
5115.389	3.8342	−0.1100	100.2	· · ·
5155.762	3.8985	−0.0900	129.5	100.9
5476.900	1.8263	−0.8900	196.3	217.6
6086.288	4.26	−0.530	79.0	73.3

Table A1
(Continued)

λ (Å)	Ex. Pot. (eV)	log gf	Equivalent Widths MJP 4112	MJP 5061
6108.125	1.68	−2.60	· · ·	99.5
6111.078	4.09	−0.810	57.9	70.4
6128.984	1.68	−3.330	· · ·	70.5
6130.141	4.26	−0.960	52.2	45.6
6133.963	4.09	−1.810	14.6	· · ·
6175.360	4.09	−0.560	73.5	70.2
6176.816	4.09	−0.260	98.2	98.3
6177.236	1.83	−3.560	30.0	43.6
6186.709	4.11	−0.920	· · ·	63.2
6327.604	1.68	−3.110	· · ·	73.2
6378.260	4.15	−0.850	68.7	54.4
6482.809	1.93	−2.830	65.0	80.1
6586.319	1.95	−2.730	76.4	74.6
6635.130	4.42	−0.740	38.4	58.0
6767.768	1.8263	−2.1700	116.2	123.9
6772.321	3.66	−0.950	· · ·	78.3
Y I				
4883.684	1.0821	−0.0100	74.1	73.0
4900.120	1.0313	−0.1300	84.6	82.6
5087.416	1.0810	−0.3100	43.6	65.0
Ba II				
4554.000	0.000	0.17	185.5	194.8
5853.700	0.000	−1.0000	67.0	· · ·
6141.700	0.000	−0.0760	123.0	144.8

REFERENCES

Anders, E., & Grevesse, N. 1989, GeCoA, 53, 197
Anthony-Twarog, B., Twarog, B., & Mayer, L. 2007, AJ, 133, 1585
Bedin, L. R., Piotto, G., Carraro, G., King, I. R., & Anderson, J. 2006, A&A, 460, L27
Bedin, L. R., et al. 2005, ApJ, 624, L45
Carney, B. W., Lee, J.-W., & Dodson, B. 2005, AJ, 129, 656
Carraro, G., Villanova, S., Demarque, P., McSwain, M. V., Piotto, G., & Bedin, L. R. 2006, AJ, 643, 1151
Chaboyer, B., Green, E. M., & Liebert, J. 1999, AJ, 117, 1360
Chen, Y. Q., Zhao, G., Nissen, P. E., Bai, G., & Qui, H. M. 2003, ApJ, 591, 925
Demarque, P., Green, E. M., & Guenther, D. B. 1992, AJ, 103, 151
Edvardsson, B., Andersen, J., Gustafsson, B., Lambert, D. L., Nissen, P. E., & Tomkin, J. 1993, A&A, 275, 101
Feltzing, S., & Gonzales, G. 2001, A&A, 367, 253
Friel, E. D., et al. 2002, AJ, 128, 2693
Garnavich, P., VandenBerg, D. A., Zurek, D. R., & Hesser, J. E. 1994, AJ, 107, 1097
Gratton, R., Bragaglia, A., Carretta, E., & Tosi, M. 2006, AJ, 642, 462
Grenon, M. 1999, Ap&SS, 265, 331
Janes, K. A. 1984, PASP, 96, 977
Johnson, H. L., & Sandage, A. R. 1955, ApJ, 121, 616
Kaluzny, J. 1990, MNRAS, 243, 492
Kaluzny, J., & Rucinski, S. M. 1995, A&AS, 114, 1
King, I. R., Bedin, L. R., Piotto, G., Cassisi, S., & Anderson, J. 2005, AJ, 130, 626
Kinman, T. D. 1965, ApJ, 142, 655
Liebert, J., Saffer, R. A., & Green, E. M. 1994, AJ, 107, 1408
Michaud, G., Richard, O., Richer, J., & VandenBerg, D. 2004, ApJ, 606, 452
Montgomery, K. A., Janes, K. A., & Phelps, R. L. 1994, AJ, 108, 585
Peterson, R. C., & Green, E. M. 1998, ApJ, 502, L39
Richard, O., Michaud, G., & Richer, J. 2002, ApJ, 580, 1110
Sandage, A. R. 1956, PASP, 68, 498
Stephens, A., & Boesgaard, A. M. 2002, AJ, 123, 1647
Stetson, P. B., Brundtt, H., & Grundahl, F. 2003, PASP, 115, 413
Tsujimoto, T., Nomoto, K., Yoshii, Y., Hashimoto, M., Yanagida, S., & Thielmann, F.-K. 1995, MNRAS, 277, 945
Vogt, S. S., et al. 1994, Proc. SPIE, 2198, 362
Worthey, G., & Jowett, K. J. 2003, PASP, 115, 96